INTERNATIONAL JOURNAL OF ADAPTIVE CONTROL AND SIGNAL PROCESSING
Int. J. Adapt. Control Signal Process. (2007)
Published online in Wiley InterScience (www.interscience.wiley.com). DOI: 10.1002/acs.994

Multiple robust track-following controller design in hard disk drives

Jongeun Choi[1,*,†], Ryozo Nagamune[2] and Roberto Horowitz[3]

[1]*Department of Mechanical Engineering, Michigan State University, East Lansing, MI 48824-1226, U.S.A.*
[2]*Department of Mechanical Engineering, University of British Columbia, Vancouver, BC, Canada V6T 1Z4*
[3]*Department of Mechanical Engineering, University of California at Berkeley, CA 94720-1742, U.S.A.*

SUMMARY

This paper presents a new technique for track-following control in hard disk drives, in order to achieve high tracking precision of magnetic read–write heads *uniformly* for a huge number of disk drives. The basic idea in this technique is to classify the disk drives into several sets depending on dynamics properties, and to apply a robust controller to each set. The problem of designing the optimal classification of dynamics and the corresponding optimal robust controllers is formulated as a nonconvex optimization problem, for which sub-optimal solutions are to be found numerically. A numerical simulation shows the usefulness of the proposed technique by illustrating a tracking performance improvement. Copyright © 2007 John Wiley & Sons, Ltd.

Received 1 October 2006; Revised 28 April 2007; Accepted 20 June 2007

KEY WORDS: multiple robust controllers; robust track-following; hard disk drives

1. INTRODUCTION

The data storage capacity in hard disk drives (HDDs) depends crucially on the achievable track-following precision of the magnetic read/write head. It is presently expected that, in order to attain 1-terabit per square inch areal storage density, which is a short-term goal in the disk drive industry, the allowable track misregistration will be 5 nm 3σ-value. This extremely high track-following performance is considered hard to achieve without sophisticated tracking servo technology.

The tracking performance has to be maintained for all HDD products, in any conceivable working condition. In other words, track-following controllers have to be designed *robustly* against

*Correspondence to: Jongeun Choi, Department of Mechanical Engineering, Michigan State University, East Lansing, MI 48824-1226, U.S.A.
†E-mail: jchoi@egr.msu.edu

Contract/grant sponsor: The Information Storage Industry Consortium (INSIC), University of California at Berkeley
Contract/grant sponsor: The Computer Mechanics Laboratory (CML), University of California at Berkeley

variations and changes of dynamics. Such dynamic variations and changes come from, for example, uneven qualities of products in batch fabrication of HDDs, the temperature changes, and quality loss due to the elapse of time. It is significant to take into account such uncertain factors in controller design.

Generally speaking, robustness and performance are incompatible requirements; robustness improvement leads to performance degradation. However, both requirements are important for track-following control in HDDs. The motivation of this paper is to provide a way to overcome this incompatibility, by designing a set of controllers that altogether give high tracking performance for a set of HDDs.

In this paper, we will propose a controller design technique for robust track-following in HDDs. The entire set of conceivable HDD dynamics is represented as a model set with polytopic parametric uncertainties. The set is partitioned into a family of polytopic subsets, and for each subset, one robust controller is designed. To design a partition of an uncertainty region and robust controllers corresponding to the partition in an optimal way, we will formulate a minimization problem of the so-called total performance. The controller design is based on a convex optimization technique. By using several controllers to partitioned regions, we can expect better tracking performance than the one obtained by a single controller.

The designed partition of the uncertainty region and robust controllers can be used in the following ways. At the end of the mass production line, for each real HDD, uncertain parameters are to be estimated off-line [1, 2] and the corresponding robust controller will be selected among the pre-designed multiple robust controllers. Alternatively, a set of pre-designed candidate controllers will be applied sequentially to each HDD and their closed-loop systems will be tested for performance specifications. A controller that provides a satisfactory performance will be selected and applied to the real HDD.

The proposed method is applicable to both single-stage and dual-stage servo systems in HDDs, and to even multi-rate control settings. Dynamic uncertainties can also be treated by the proposed method if such uncertainties are parameterized with a finite number of variables.

2. POLYTOPIC PARAMETRIC UNCERTAIN LTI SYSTEMS

First of all, we will introduce a general mathematical representation that encompasses a typical disk drive model for servo control. Let us consider a discrete time[‡] linear time invariant (LTI) generalized plant with parametric uncertainty $\lambda \in \Lambda$, in short denoted by Σ^{λ}, as depicted in Figure 1,

$$\begin{bmatrix} z \\ y \end{bmatrix} = \left[\begin{array}{c|cc} A^{\lambda} & B_1^{\lambda} & B_2^{\lambda} \\ \hline C_1^{\lambda} & D_{11}^{\lambda} & D_{12}^{\lambda} \\ C_2 & D_{21} & 0 \end{array}\right] \begin{bmatrix} w \\ u \end{bmatrix}, \quad A^{\lambda} \in \mathbb{R}^{n \times n} \tag{1}$$

[‡]We only consider the discrete-time case here but the application to the continuous-time case is straightforward.

DOI: 10.1002/acs

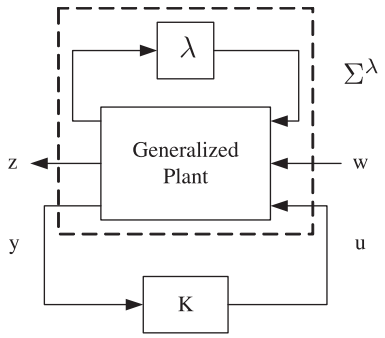

Figure 1. A generalized plant with parametric uncertainty λ (denoted by Σ^{λ}) and a controller K.

where $z \in \mathbb{R}^{n_z}$ is the output of the system, $w \in \mathbb{R}^{n_w}$ the disturbance to the system, $u \in \mathbb{R}^{n_u}$ the control action, $y \in \mathbb{R}^{n_y}$ the measured output, and

$$\left[\begin{array}{c|c} A & B \\ \hline C & D \end{array}\right] := D + C(zI - A)^{-1}B \tag{2}$$

Here, the superscript 'λ' on a matrix means that the matrix is a function of an uncertain parameter vector λ. The set of all uncertain plants with $\lambda \in \Lambda$ is denoted as Σ^{Λ} given by the formula

$$\Sigma^{\Lambda} := \{\Sigma^{\lambda} : \lambda \in \Lambda\} \tag{3}$$

Assumptions on the plant parameters are (A.1) $(A^{\lambda}, B_2^{\lambda}, C_2)$ is stabilizable and detectable for each $\lambda \in \Lambda$; (A.2) Λ is a convex polytope; (A.3) the system matrix in Equation (1) is affine in λ. The first assumption (A.1) is necessary and sufficient for each system in Σ^{Λ} to be stabilizable with dynamic output feedback. (A.2) and (A.3) are necessary for robust controller design based on LMI techniques (see more details in [3–5]).

3. PROBLEM FORMULATION

Consider the set Σ^{Λ} of parametric uncertain LTI systems, each of which is represented in Equation (1). We would like to simultaneously determine (1) a partition[§] $\{\Lambda_q : q \in \mathscr{Z}_N\}$ of Λ, and (2) synthesize a set of robust controllers $\{K_q : q \in \mathscr{Z}_N\}$, where K_q is applied to the set Σ^{Λ_q}, such that a certain worst-case performance cost (to be defined below) is minimized. The set of robust

[§]For a given compact and closed parameter set Λ, we call $\{\Lambda_q : q \in \mathscr{Z}_N\}$ *a partition* of a set Λ, where $\mathscr{Z}_N$ is the set of N coordinates of the partition, if $\Lambda_q \subset \Lambda$ is nonempty, closed, and satisfies

$$\bigcup_{q \in \mathscr{Z}_N} \Lambda_q = \Lambda \quad \text{and} \quad \text{Int}(\Lambda_i) \cap \text{Int}(\Lambda_j) = \emptyset \ \text{ for } i \neq j \tag{4}$$

where $\text{Int}(\Lambda_i)$ is the interior of the set Λ_i. In other words, a partition of a set Λ is a collection of nonempty subsets of Λ whose interior is disjoint and whose union is all of Λ.

DOI: 10.1002/acs

controller's coordinates is denoted as $\mathscr{Z}_N$, and let the coordinate of a robust controller be also the coordinate of the corresponding subset of the partition.

The regional controller K_q will be designed to regulate any linear uncertain system in the uncertain plant set Σ^{Λ_q}. Given a proper real-rational controller $K_q(z)$ for uncertain systems Σ^{Λ_q}

$$K_q(z) := \left[\begin{array}{c|c} A_{K_q} & B_{K_q} \\ \hline C_{K_q} & D_{K_q} \end{array}\right], \quad A_{K_q} \in \mathbb{R}^{n\times n} \tag{5}$$

a realization of the closed-loop transfer function from the disturbance signal w to the output signal z is denoted by $T_{zw}(\lambda, K_q)$. We define several performance measures. For a given set of uncertain LTI systems Σ^{Λ_q} and a robustly stabilizing controller K_q, we define the *worst-case performance cost* of the uncertain closed-loop systems by

$$J_2(\Lambda_q, K_q) := \sup_{\lambda\in\Lambda_q} \|T_{zw}(\lambda, K_q)\|_2 \tag{6}$$

where $\|\cdot\|_2$ denotes the $\mathscr{H}_2$ norm. The *total performance* is defined as the maximum of such worst-case performance of each local region given by

$$\max_{q\in\mathscr{Z}_N} J_2(\Lambda_q, K_q) \tag{7}$$

We are interested in minimizing the total performance, which sets an upper bound on the performance of an individual closed-loop system. Next, the total performance minimization problem is formally stated.

Problem

For a given set of uncertain LTI systems Σ^{Λ} with a convex polytope Λ and a given coordinate $\mathscr{Z}_N$, design a partition $\{\Lambda_q : q \in \mathscr{Z}_N\}$ of the uncertainty set Λ and a set of stabilizing robust controllers $\{K_q : q \in \mathscr{Z}_N\}$, such that the total performance is minimized, i.e. solve the optimization problem

$$\min_{\{\Lambda_q\},\{K_q\in\mathscr{K}(\Lambda_q)\}} \left[\max_{q\in\mathscr{Z}_N} J_2(\Lambda_q, K_q)\right] \tag{8}$$

where $\mathscr{K}(\Lambda_q)$ is the set of all controllers that internally stabilize the closed-loop system for all $\lambda\in\Lambda_q$.

The formulated optimization is nonconvex, and thus, it is hard to solve exactly in the global optimal sense. In the following section, we will explain how to get a reasonable solution in a systematic way.

4. DESIGN OF A PARTITION AND MULTIPLE CONTROLLERS

First, we show how to partition a convex polytopic uncertainty set into a smaller set of convex polytopic uncertainty regions using the Cartesian product. The imposition of the constraint on a partition that it must have convex polytopic subsets, simplifies the tasks of determining partitions of uncertain systems as well as their respective sets of multiple robust controllers. Subsequently, we discuss the design of a set of robust controllers. Finally, a descent search algorithm for the optimization given by Equation (8) will be presented.

DOI: 10.1002/acs

4.1. Partitioning the polytopic uncertainty

Recall the uncertain parameter $\lambda(\cdot) : \mathbb{Z}_+ \to \Lambda$. Suppose that Λ consists of two parameter subspaces, one of which is to be partitioned while the other is not, i.e. $\lambda := [\lambda^{*\mathrm{T}} \lambda_*^{\mathrm{T}}]^{\mathrm{T}} \in \Lambda \subset \mathbb{R}^u$, where $\lambda^* \in \Lambda^* \subset \mathbb{R}^{\bar{u}}$, $\lambda_* \in \Lambda_* \subset \mathbb{R}^{\underline{u}}$, and $\bar{u} + \underline{u} = u$. The partitioning of Λ^* is assumed to be of importance to enhance the performance of the closed-loop system, i.e. there is significant improvement if we partition Λ^* into multiple subsets. On the other hand, the parameter $\lambda_* \in \Lambda_*$ is not measured or estimated, since it may not be possible to estimate this parameter and/or it may not significantly affect the robust performance of the closed-loop system.

Now we present a useful technique for partitioning the entire uncertainty into a collection of convex polytopes: the Cartesian product partition technique.

Suppose the parameter set is contained in a hyper-rectangular

$$\Lambda^* \subseteq \prod_{i=1}^{\bar{u}} [\lambda_i^{\min}, \lambda_i^{\max}] \tag{9}$$

where $\Lambda^* \in \mathbb{R}^{\bar{u}}$ and the notation $\prod$ denotes the Cartesian product. Let each closed interval be partitioned as

$$\lambda_i^{\min} = \delta_0^i < \delta_1^i < \cdots < \delta_{N_i-1}^i < \delta_{N_i}^i = \lambda_i^{\max} \tag{10}$$

where N_i is the number of sections in the ith coordinate of Λ^*. Define the coordinate of the subsets in the partition (and its respective controllers) as a $\bar{u}$-tuple of positive integers

$$q := (q_1, \ldots, q_{\bar{u}}) \in \mathscr{Z}_N \subset \mathbb{Z}_+^{\bar{u}} \tag{11}$$

where $\mathscr{Z}_N$ is denoted by

$$\mathscr{Z}_N := \prod_{i=1}^{\bar{u}} \mathscr{Z}_{N_i} \tag{12}$$

to be the set of all $\bar{u}$-tuples of elements of q such that $q_i \in \mathscr{Z}_{N_i} := \{1, 2, \ldots, N_i\}$ for each i. The number of total subsets in the parametric uncertainty partition is $N := N_1 \cdot N_2 \ldots N_{\bar{u}}$. Finally, we define the intersection of the Cartesian product of the indexed family and Λ^*, denoted by Λ_q^*

$$\Lambda_q^* := \prod_{i=1}^{\bar{u}} [\delta_{q_i-1}^i, \delta_{q_i}^i] \cap \Lambda^* \tag{13}$$

to be the set of all $\bar{u}$-tuples of elements of Λ^* such that $\lambda_i \in [\delta_{q_i-1}^i, \delta_{q_i}^i]$ and $\lambda_i \in \lambda_i^*$, where λ_i^* is the ith element of λ^*, for each i. Notice that $\Lambda_q := \Lambda_q^* \times \Lambda_*$ is a nonempty closed convex set. A simple example of the sets Λ_q is illustrated in Figure 2. By choosing appropriate δ_j^i in Equation (10), Λ_q satisfies the conditions in Equation (4). The elements in a subset of borders $\{\delta_k^i : k \in \mathscr{Z}_{N_i}\} \backslash \{\delta_0^i, \delta_{N_i}^i\}$ for $i \in \{1, \ldots, \bar{u}\}$ in Equation (10) are the optimization parameters.

DOI: 10.1002/acs

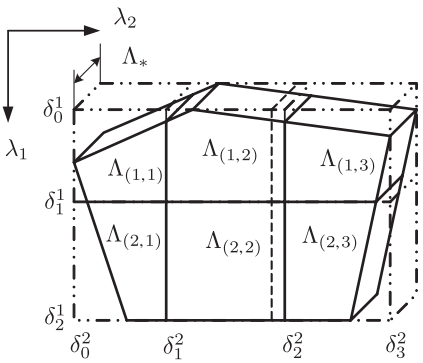

Figure 2. A Cartesian product partition (solid line) and a locally updated partition (dotted line) for optimization.

4.2. Robust $\mathscr{H}_2$ controller design for a fixed partition

For a given convex polytopic subset Λ_q, a sub-optimal robust controller shall be designed. Let us parameterize the qth controller K_q in Equation (5) by defining a matrix Θ_q as

$$\Theta_q := \begin{bmatrix} A_{K_q} & B_{K_q} \\ C_{K_q} & D_{K_q} \end{bmatrix} \in \mathbb{R}^{(n+n_u)\times(n+n_y)} \tag{14}$$

Then, as in [6], the closed-loop system matrix with $\lambda \in \Lambda_q$ can be written in terms of Θ_q

$$\begin{bmatrix} A_{\mathrm{cl}}^{\lambda}(\Theta_q) & B_{\mathrm{cl}}^{\lambda}(\Theta_q) \\ C_{\mathrm{cl}}^{\lambda}(\Theta_q) & D_{\mathrm{cl}}^{\lambda}(\Theta_q) \end{bmatrix} := \begin{bmatrix} A_0^{\lambda} & B_0^{\lambda} \\ C_0^{\lambda} & D_{11}^{\lambda} \end{bmatrix} + \begin{bmatrix} \mathscr{B}^{\lambda} \\ \mathscr{D}_{12}^{\lambda} \end{bmatrix} \Theta_q [\mathscr{C} \;\; \mathscr{D}_{21}] \tag{15}$$

where

$$\begin{gathered} A_0^{\lambda} := \begin{bmatrix} A^{\lambda} & 0_{n\times n} \\ 0_{n\times n} & 0_{n\times n} \end{bmatrix}, \quad B_0^{\lambda} := \begin{bmatrix} B_1^{\lambda} \\ 0_{n\times n_w} \end{bmatrix}, \quad C_0^{\lambda} := [C_1^{\lambda} \;\; 0_{n_z\times n}] \\ \mathscr{B}^{\lambda} := \begin{bmatrix} 0_{n\times n} & B_2^{\lambda} \\ I_{n\times n} & 0_{n\times n_u} \end{bmatrix}, \quad \mathscr{C} := \begin{bmatrix} 0_{n\times n} & I_{n\times n} \\ C_2 & 0_{n_y\times n} \end{bmatrix}, \quad \mathscr{D}_{12}^{\lambda} := [0_{n_z\times n} \;\; D_{12}^{\lambda}] \\ \mathscr{D}_{21} := \begin{bmatrix} 0_{n\times n_w}, & D_{21} \end{bmatrix} \end{gathered} \tag{16}$$

Now we present an algorithm for finding a robustly stabilizing controller matrix Θ_q that solves

$$\min_{\Theta_q} \max_{\lambda\in\Lambda_q} \|T_{zw}(\lambda, \Theta_q)\|_2 \tag{17}$$

Equation (17) is equivalent to solving an optimization problem over the standard matrix inequality conditions for $\mathscr{H}_2$ norm [7, 8]:

$$\min_{W_q, P_q, \Theta_q, \gamma_q^2} \gamma_q^2 \quad \text{s.t. } \mathscr{M}(W_q, P_q, \Theta_q, \lambda, \gamma_q) \succ 0 \;\text{ for } \lambda \in \mathscr{V}(\Lambda_q) \tag{18}$$

DOI: 10.1002/acs

Here, $\mathscr{M}(W_q, P_q, \Theta_q, \lambda, \gamma_q)$ is given by

$$\mathscr{M}(W_q, P_q, \Theta_q, \lambda, \gamma_q)$$

$$:= (\gamma_q^2 - \mathrm{trace}(W_q)) \oplus \begin{bmatrix} W_q & C_{\mathrm{cl}}^{\lambda}(\Theta_q) P_q & D_{\mathrm{cl}}^{\lambda}(\Theta_q) \\ \star & P_q & 0 \\ \star & \star & I \end{bmatrix} \oplus \begin{bmatrix} P_q & A_{\mathrm{cl}}^{\lambda}(\Theta_q) P_q & B_{\mathrm{cl}}^{\lambda}(\Theta_q) \\ \star & P_q & 0 \\ \star & \star & I \end{bmatrix}$$

where $\star$ represents entries that follow from symmetry, and $\oplus$ denotes the direct sum of matrices. P_q and W_q are matrices of appropriate size satisfying $P_q = P_q^{\mathrm{T}}$ and $W_q = W_q^{\mathrm{T}}$. $A_{\mathrm{cl}}^{\lambda}$, $B_{\mathrm{cl}}^{\lambda}$, $C_{\mathrm{cl}}^{\lambda}$, and $D_{\mathrm{cl}}^{\lambda}$ are defined in Equation (15).

Due to the uncertain parameter λ in the closed-loop system matrix in Equation (15), the closed-loop matrix as in Equation (15) is convex for $\lambda \in \Lambda$, and therefore, the infinite number of matrix inequalities $\mathscr{M}(\ldots, \lambda) \succ 0$, where $\lambda \in \Lambda_q$, becomes a finite number of matrix inequalities $\mathscr{M}(\ldots, \lambda) \succ 0$, where $\lambda \in \mathscr{V}(\Lambda_q)$. This problem is, however, nonconvex, due to the coupling term between P_q and Θ_q in Equation (18). A similar descent algorithm to the one used in [9], which utilizes the coordinate descent method for designing a $\mathscr{H}_2$ controller, is adopted for finding sub-optimal $\mathscr{H}_2$ controllers.

4.3. Synthesis of a partition with its respective set of robust controllers

Our main problem is to solve the following optimization:

$$(\{\Lambda_q^{\mathrm{opt}}\}, \{\Theta_q^{\mathrm{opt}}\}) := \arg \min_{\{\Lambda_q\}, \{\Theta_q \in \mathscr{K}(\Lambda_q)\}} \left[\max_{q \in \mathscr{Z}_N} J_2(\Lambda_q, \Theta_q) \right] \tag{19}$$

The following assumptions are introduced to develop an algorithm for solving the optimization problem in Equation (19). (B.1) A partition of the uncertainty set $\{\Lambda_q\}$ is well chosen so that the optimization in Equation (18) is feasible for any given subset Λ_q. (B.2) The nonconvex optimization problem in Equation (18) can be solved, and we denote $\hat{\Theta}_q$ as the *optimal* solution for a given subset Λ_q. (B.3) The optimal performance cost $\hat{\gamma}_q$ continuously changes with respect to the changes in the subset Λ_q. Here, $\hat{\gamma}_q$ is computed from the *optimal* controller $\hat{\Theta}_q$: $\hat{\gamma}_q := \max_{\lambda \in \Lambda_q} \|T_{zw}(\lambda, \hat{\Theta}_q)\|_2$. The assumptions allow us to devise a descent synthesis algorithm to design a partition and multiple controllers. The feasibility of the assumptions will be discussed shortly. We now denote Λ_q^j as a given qth region of the partition at the iteration time j, and $\hat{\Theta}_q^j$ and $\hat{\gamma}_q^j$ (or $\hat{\gamma}(\Lambda_q^j)$) as the corresponding optimal controller and resulting performance cost, respectively. Then we have a following fact.

Lemma 1

Let $\hat{\gamma} : \Lambda \to \mathbb{R}$ be a function from a given partitioned subset in Λ to the optimized performance cost in $\mathbb{R}$, then the function $\hat{\gamma}$ is continuous and monotone, i.e. whenever $\Lambda_q^j \subset \Lambda_q^{j+1}$ then $\hat{\gamma}(\Lambda_q^j) < \hat{\gamma}(\Lambda_q^{j+1})$.

Proof

Continuity is given by assumption (B.3). Monotonicity is guaranteed by the nature of the optimization, due to the inclusion relationship $\Lambda_q^j \subset \Lambda_q^{j+1}$. □

DOI: 10.1002/acs

Now we present an algorithm to solve the main optimization problem in Equation (19).

1. [*Initial Design of* $\{\Lambda_q\}$ *and* $\{\Theta_q\}$]: Set $\{\Lambda_q^1\}$ and $\{\Theta_q^1\}$ to the initial designs. Also set $\{\gamma_q^1\}$ to the performance cost in Equation (18) and set $j = 1$.
2. [*Design of* $\{\Lambda_q\}$]: Update the partition $\{\Lambda_q^j\}$ so that the worst performance region should be reduced. Denote the set of coordinates of partitioned regions that produce the maximum total performance cost by

$$L^j := \arg \max_{q \in \mathscr{Z}_N} \gamma_q^j \tag{20}$$

   Select an element $l^j \in L^j$ and shrink this 'loser set' by $\Lambda_{lj}^{j+1} = \Lambda_{lj}^j \backslash \delta\Lambda$ and a neighboring subset takes $\delta\Lambda$. In doing so, make sure that the updated subsets and the subsets in the previous iteration are subject to the constraint

$$\Lambda_{lj}^{j+1} \subset \Lambda_{lj}^j, \quad \Lambda_q^{j+1} \supseteq \Lambda_q^j \quad \text{or} \quad \Lambda_q^{j+1} \subseteq \Lambda_q^j, \ \ q \in \mathscr{Z}_N \backslash l^j \tag{21}$$

3. [*Design of* $\{\Theta_q\}$]: Design *sub-optimal* robust controllers for the updated subsets $\{\Lambda_q^{j+1} : q \in \mathscr{Z}_N\}$ and evaluate the resulting worst-case cost set $\{\gamma_q^{j+1} : q \in \mathscr{Z}_N\}$. Since $\Lambda_{lj}^{j+1} \subset \Lambda_{lj}^j$, we expect that $\gamma_{lj}^{j+1} < \gamma_{lj}^j$.
4. Iterate Steps 2 and 3 while keeping $\gamma_{k \in L^j}^j \geqslant \gamma_q^{j+1}$ for $q \in \mathscr{Z}_N \backslash l^j$ by selecting a sufficiently small set $\delta\Lambda$. Continue this iteration until $\gamma_{q \in L^j}^j$ converges.

In each iteration, we compute the set L^j and update the partition and its controllers. In this way we can improve the total performance cost as the iteration time increases.

Unfortunately, these optimization problems are nonconvex and so assumption (B.2) may not be satisfied. Given the current state of robust control theory, we cannot compute the optimal solution $\hat{\Theta}_q$ for a given polytopic uncertain set Λ_q [7]. Therefore, in this paper, only a sub-optimal controller is computed as explained in the previous section. However, if the sub-optimal controller continuously changes with respect to the changes in the subset Λ_q, then assumption (B.3) holds, since the worst-case performance is the continuous function of the controller and the uncertainty simultaneously. Therefore, we can always find a sufficiently small set $\delta\Lambda$ so that the inequality in Step 4 holds in order to improve the total performance as the iteration time increases.

Given the Cartesian product partition technique previously described, it is easy to update the partition subject to the inclusion and exclusion constraint, Equation (21), as shown in Figure 2. For example, assume that $q = (1, 2)$ is the 'loser index' that has the maximum performance cost among $q \in \mathscr{Z}_N$. After updating the partition as illustrated with a dotted line in Figure 2, we have $\Lambda_q^{j+1} \subset \Lambda_q^j$ for $q \in \{(1, 2), (2, 2)\}$ and $\Lambda_q^{j+1} \supset \Lambda_q^j$ for $q \in \{(1, 3), (2, 3)\}$. Therefore, γ_q^{j+1} for $q \in \{(1, 2), (2, 2)\}$ are expected to decrease while γ_q^{j+1} for $q \in \{(1, 3), (2, 3)\}$ are expected to increase.

The presented optimization problem in Equation (8) is somewhat similar to the encoder and decoder design problem in the vector quantization theory [10]. The encoder design is replaced by partitioning the compact parametrically uncertain set, and the decoder design is replaced by the optimization of a robust controller for each local subset. Finally, the usual quantization error cost is exchanged with the worst-case $\mathscr{H}_2$ performance cost of the closed-loop system with respect to any parameter variations within the uncertainty.

DOI: 10.1002/acs

5. AN ILLUSTRATIVE EXAMPLE

5.1. The generalized plant

We now synthesize multiple robust controllers for a dual-stage HDD servo with a translational MEMS actuated slider, shown as the block diagram in Figure 3. The main actuator for this system is a voice coil motor (VCM) and the secondary actuator is a microactuator (MA). The control inputs are u_v and u_m, respectively, for the VCM and the MA. The signals y_h, y_p, y_v, and y_m are, respectively, the read/write head position, the output of a strain sensor mounted on the suspension, the suspension tip displacement, and the position of the MA relative to the suspension tip displacement. y_{PES} is the position error signal (PES), which is defined as the position of the read/write head with respect to the track. w_v is the normalized white Gaussian airflow disturbance to the VCM. The controller has access to measurements of y_p, y_m, and y_{PES}, each of which is contaminated by its respective white Gaussian measurement noise signal. We only consider three important modes of the VCM reducing the order of the generalized plant. The transfer functions for the VCM dynamics, G_{V}, the MA dynamics, G_{M}, and the coupling between the VCM and MA dynamics, G_{C}, can be represented as

$$G_{\mathrm{V}}(s) := \sum_{i=1}^{3} \frac{A_i}{s^2 + 2\zeta_i \omega_i s + \omega_i^2}, \quad G_{\mathrm{M}}(s) := \frac{A_m}{s^2 + 2\zeta_m \omega_m s + \omega_m^2}$$
$$G_{\mathrm{C}}(s) := \frac{2\zeta_m \omega_m s + \omega_m^2}{s^2 + 2\zeta_m \omega_m s + \omega_m^2} \tag{22}$$

where A_i and A_m are static gain matrices for $G_{\mathrm{V}}(s)$ and $G_m(s)$, respectively, given by

$$A_i := \begin{bmatrix} a_{w_v \to y_p} & a_{u_v \to y_p} \\ a_{w_v \to y_v} & a_{u_v \to y_v} \end{bmatrix} \quad \text{for } i \in \{1, 2, 3\}, \qquad A_m := [a_{u_m \to y_m}]$$

and all parameters in Equation (22) are as listed in Table I. The track runout signal, r, models the head motion relative to the tracks on the disk resulting from mechanical imperfections, D/A

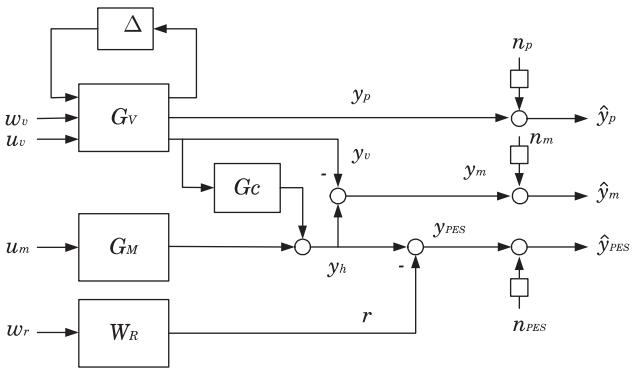

Figure 3. The block diagram of the dual-stage HDD servo with a translational MEMS actuated slider.

DOI: 10.1002/acs

Table I. Nominal parameter values.

q	Mode	Parameter		
		ζ_q	ω_q	A_q
1	Rigid body and friction mode	0.5	376.99	$\begin{bmatrix} 0 & 0 \\ 0 & 1.4 \times 10^4 \end{bmatrix}$
2	Butterfly mode	0.015	4.6496×10^4	$\begin{bmatrix} -0.439 & 0.48 \\ 0.768 & -0.84 \end{bmatrix}$
3	Sway mode	0.015	6.7218×10^4	$\begin{bmatrix} -0.783 & 0.041 \\ 0.576 & -0.3 \end{bmatrix}$
m	Microactuator	0.2	1.4137×10^4	[0.2]

quantization noise, and power-amp noise. The low-frequency nature of track runout $W_{\mathrm{R}}(s)$ is characterized as

$$r(s) := \frac{1.2 \times 10^5 s^2 + 2.89 \times 10^9 s + 5.298 \times 10^{12}}{s^3 + 2684 s^2 + 1.756 \times 10^6 s + 4.703 \times 10^8} w_r(s)$$

where $w_r(s)$ is normalized white Gaussian noise. The inputs and outputs of the generalized plant shown in Figure 1, are chosen as

$$z := \begin{bmatrix} y_{\mathrm{PES}} \\ u_v \\ 0.01 u_m \end{bmatrix}, \quad w := \begin{bmatrix} w_r \\ w_v \\ n_{\mathrm{PES}} \\ n_m \\ n_p \end{bmatrix}, \quad y := \begin{bmatrix} \hat{y}_{\mathrm{PES}} \\ \hat{y}_m \\ \hat{y}_p \end{bmatrix}, \quad u := \begin{bmatrix} u_v \\ u_m \end{bmatrix}$$

where $\hat{q}$ denotes the measurement of the signal q contaminated by measurement noise. n_{PES}, n_m, and n_p are normalized white Gaussian signals that will be scaled to produce the measurement noises for $\hat{y}_{\mathrm{PES}}$, $\hat{y}_m$, and $\hat{y}_p$, respectively. The block diagram in Figure 3 shows interconnections among transfer functions, an uncertain block, and input and output channels. The values of ζ_2 and ζ_3 in Equation (22) and Table I are allowed to vary by up to $\pm 15\%$, while ω_2 and ω_3 are allowed to vary by up to $\pm 1\%$. It is assumed that the variations in $2\zeta_2\omega_2$ and $2\zeta_3\omega_3$ are correlated and so are those in ω_2^2 and ω_3^2. With these simplifying assumptions, the generalized model only contains two parametric uncertainties. Let λ_1 correspond to the variations in $2\zeta_i w_i$ and λ_2 represent the variations in w_i^2. Figure 5 shows the open-loop bode plots from u_v to y_{PES} and u_m to y_{PES} for 160 randomly selected values of $\lambda \in \Lambda$. The 11th order, generalized plant with parametric uncertainties, denoted by Σ^λ, for the robust controller synthesis is shown in Figure 1. Σ^λ is obtained by discretizing the nominal plant using a zero-order hold and assuming that the effect of λ is the same in discrete time with a fast sampling time of 4×10^{-5} s.

DOI: 10.1002/acs

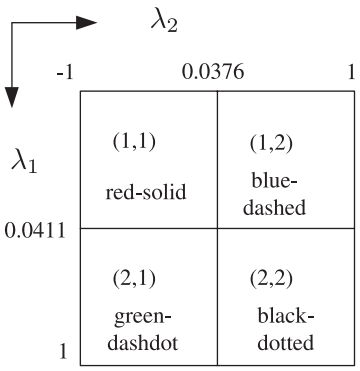

Figure 4. The final partition, its coordinates and a legend for the randomly generated parameters.

Table II. Worst-case costs achieved by the multiple robust controllers.

$\gamma_{(1,1)} = 8.71$	$\gamma_{(1,2)} = 8.78$
$\gamma_{(2,1)} = 8.78$	$\gamma_{(2,2)} = 8.80$

5.2. *Synthesis of controllers*

For this example, we found a *single* robust controller K_{single} based on the coordinate descent method (P–K iteration) [9, 11], achieving an upper bound of $\gamma_{\text{single}} = 9.10$ for the entire uncertainty region using the algorithm explained in Section 4.2. Next we found a Cartesian product partition (two by two) as shown in Figure 4 and its *multiple* controllers $\{K_q : q \in \mathscr{Z}_N\}$ using the optimization algorithm elaborated in Section 4.3. The previously found single controller K_{single} served as initial controllers and the equally spaced partition was chosen as the initial partition for the nonconvex optimization as in Equation (19). The optimization highly depends on initial conditions and the problem structure. The upper bounds achieved by multiple controllers are shown in Table II with respect to the coordinates of the partition. The overall optimization that includes synthesis of a single controller and multiple controllers, took about a couple of hours using a high-end commercial computer with Intel® *Core*™ 2 *Duo* Processor E6700 (2.66 GHz, 1066 FSB).

As shown in Table II, the total performance cost is $\gamma_{\text{total}} := \max_{q \in \mathscr{Z}_4} \gamma_q = 8.80$, which improves the cost obtained by the single controller $\gamma_{\text{single}} = 9.10$ by 3.36%.

5.3. *Performance evaluation*

In order to evaluate the closed-loop uncertain systems, 160 perturbed systems were generated by parameters sampled from two independent uniform probability density functions. These randomly generated open-loop transfer functions from u_v and u_m to y_{PES} are plotted in Figure 5. Each randomly generated open-loop plant from u_v to y_{PES} is classified and plotted according to the subset of the partition where it is contained as shown in Figure 6.

- The 31 plants that belong to $\Lambda_{(1,1)}$ are plotted with red solid lines.
- The 45 plants that belong to $\Lambda_{(1,2)}$ are plotted with blue dashed lines.

DOI: 10.1002/acs

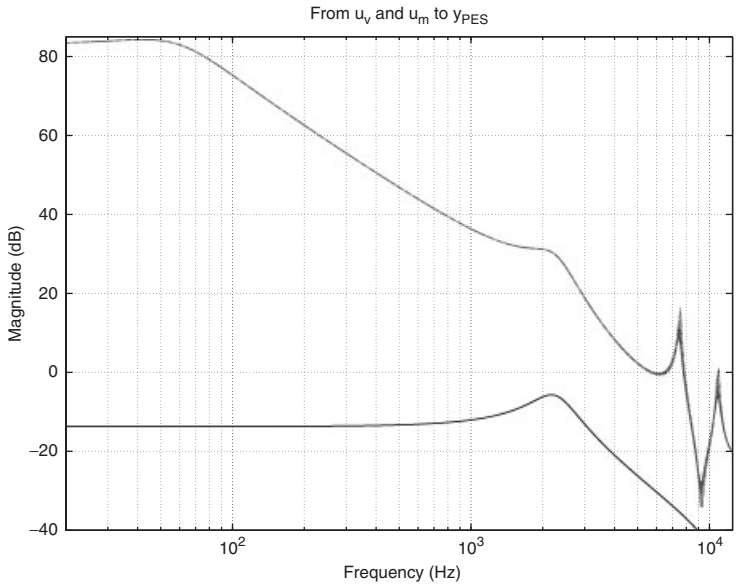

Figure 5. The perturbed bode plots of transfer functions from u_v and u_m (black solid line) to y_{PES}.

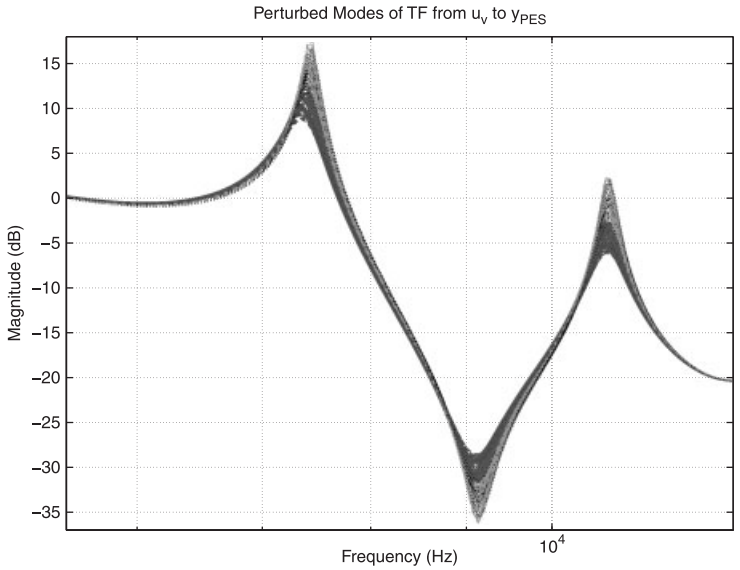

Figure 6. Sixty randomly generated transfer functions from u_v to y_{PES}, a closed look at the second and third suspension modes.

- The 48 plants that belong to $\Lambda_{(2,1)}$ are plotted with green dash-dotted lines, and
- the 36 plants that belong to $\Lambda_{(2,2)}$ are plotted with black dotted lines.

DOI: 10.1002/acs

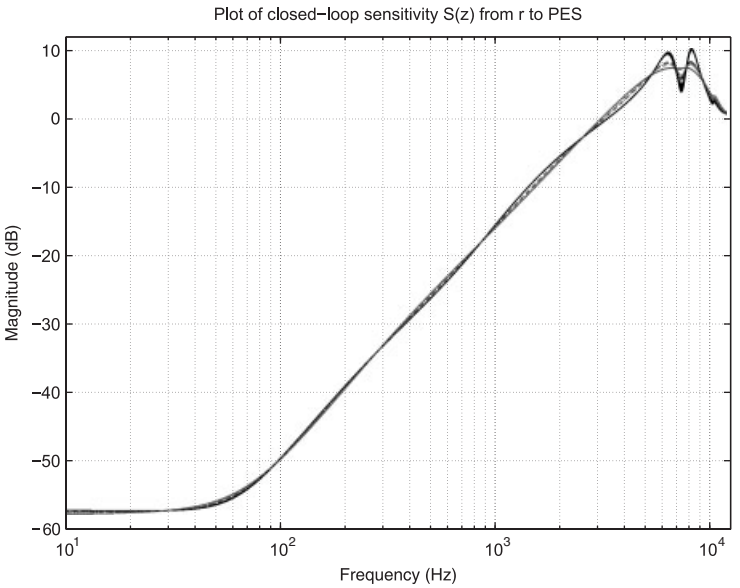

Figure 7. Sensitivity functions of the perturbed closed-loop systems with *the single controller* (black solid line) and with *the multiple controllers* (see the legend in Figure 4).

Table III. Comparison of nominal and worst-case closed-loop RMS values of $\sqrt{z^{\mathrm{T}}z}$, the PES, u_v, and u_m from sensitivity functions based on the single robust controller and the multiple robust controllers.

	$\sqrt{z^{\mathrm{T}}z}$		PES (nm)		u_v (mV)		u_m (mV)	
Design approach	Nominal	WC	Nominal	WC	Nominal	WC	Nominal	WC
K_{single}	8.975	9.026	8.326	8.352	1.058	1.066	317.88	325.1
$K_{(1,1)}$	8.706	8.706	8.117	8.117	1.087	1.088	295.35	295.43
$K_{(1,2)}$	8.766	8.765	8.168	8.168	1.062	1.066	299.84	299.71
$K_{(2,1)}$	8.733	8.763	8.139	8.151	1.075	1.081	297.62	303.08
$K_{(2,2)}$	8.752	8.782	8.156	8.168	1.067	1.073	299.03	304.23
Max of WC	n/a	8.782	n/a	8.168	n/a	1.088	n/a	304.23

These closed-looped sensitivity functions $S(z)$ from r to the controlled output y_{PES} by the single controller K_{single} and multiple controllers $\{K_q : q \in \mathscr{Z}_4\}$ are plotted in Figure 7. It is clearly seen that the sampled sensitivity transfer functions by the partition and its multiple controllers have much lower peak gains as compared with the one achieved by a single controller as shown in Figure 7.

Table III summarizes nominal and worst-case RMS values of $\sqrt{z^{\mathrm{T}}z}$, the PES, u_v, and u_m from closed-loop generalized plants based on the single robust controller and the multiple robust controllers. For the nominal plant and randomly generated plants, single and multiple controllers were evaluated by measuring $\mathscr{H}_2$ norms of closed-loop generalized plants. The multiple controller

DOI: 10.1002/acs

scheme improves the variance of z channel by 2.5 and 2.7% in terms of the nominal and worst-case performances, respectively. It also improves the variance of the PES signal by 2 and 2.2% in nominal and worst-case performances. The variance of u_m is improved by 5.9 and 6.4% in nominal and worst-case performances. There is degradation in the variance of u_v by 0.9%, 2.0% in nominal and worst-case performances sense utilizing the multiple robust controllers, but we should recall that the performance channel was chosen as z. As expected from the optimization costs achieved in Table II, most maxima of worst-case performances were obtained in the coordinate of (2, 2).

6. CONCLUSIONS

In this paper, we have proposed the design of multiple robust track-following controllers for HDDs. The designed multiple controllers are useful in achieving uniformly high tracking precision of the read/write head for hundreds of thousands of disk drives, as well as in maintaining such high precision even in the face of dynamic changes among disk drives due to the limited manufacturing tolerance. One simulation example has been provided to illustrate that multiple robust controllers can improve the tracking performance compared with a single robust controller. The performance improvement depends highly on parametric uncertainty types. For instance, if we deal with large parametric uncertainty of the natural frequencies in butterfly modes, the resulting improvement by using multiple robust controllers can be much greater.

We remark that other LMI formulations, such as the formulation using the parameter-dependent Lyapunov function in [8], as well as the formulation for multirate controller design, can also be utilized in the design of multiple robust controllers for further performance improvement [5, 9]. However, such formulations increase the computational cost, and therefore, are applicable to only small sizes of servo problems with the current computer power.

We are currently developing controller selection algorithms for a given plant generated by the mass production manufacturing process. Once we develop such algorithms, the proposed method can be applied to real disk drive production immediately.

ACKNOWLEDGEMENTS

The authors would like to thank Mr Richard Conway at the University of California, Berkeley, for allowing them to use his GUI software for constructing the model of hard disk drives. We also appreciate reviewers' valuable comments on this paper.

REFERENCES

1. Ljung L. *Theory and Practice of Recursive Identification*. The MIT Press: Cambridge, MA, 1983.
2. Wolodkin G, Rangan S, Poollar K. An LFT approach to parameter estimation. *Proceedings of the American Control Conference*, 1997; 2088–2284.
3. Scherer C, Gahinet P, Chilali M. Multiobjective output-feedback control via LMI optimization. *IEEE Transactions on Automatic Control* 1997; **42**(7):896–911.
4. Gahinet P, Nemirovski A, Laub AJ, Chilali M. *LMI Control Toolbox User's Guide*. The Mathworks Inc.: Natick, MA, 1995.
5. Choi J, Nagamune R, Horowitz R. Multiple robust controller design based on parameter dependent Lyapunov functions. *Proceedings of the 17th International Symposium on Mathematical Theory of Networks and Systems*, Kyoto, Japan, 2006.

DOI: 10.1002/acs

6. Gahinet P, Apkarian P. A linear matrix inequality approach to H_∞ control. *International Journal of Robust and Nonlinear Control* 1994; **40**:421–448.
7. Kanev S, Scherer C, Verhaegen M, De Shutter B. Robust output-feedback controller design via local BMI optimization. *Automatica* 2004; **40**:1115–1127.
8. de Oliveira MC, Geromel JC, Bernussou J. Extended H_2 and H_∞ norm characterizations and controller parameterizations for discrete-time systems. *International Journal of Control* 2002; **75**(9):666–679.
9. Nagamune R, Huang X, Horowitz R. Robust control synthesis techniques for multirate and multi-sensing track-following servo systems in hard disk drives. *Journal of Dynamic Systems*, *Measurement and Control* (ASME), in press.
10. Gersho A, Gray RM. *Vector Quantization and Signal Compression*. Kluwer Academic Publishers: Dordrecht, 2001.
11. Choi J, Nagamune R, Horowitz R. Synthesis of multiple robust controllers for parametric uncertain LTI systems. *Proceedings of the 25th American Control Conference*, Minneapolis, MN, U.S.A., 2006.

DOI: 10.1002/acs